Pergamon

Applied Thermal Engineering Vol. 18, Nos 3–4, pp. 157–169, 1998

Printed in Great Britain

PII: S1359-4311(97)00024-0

1359-4311/98 $19.00 + 0.00

CONVECTIVE HEAT TRANSPORT OF HIGH-PRESSURE FLOWS INSIDE ACTIVE, THICK WALLED-TUBES WITH ISOTHERMAL OUTER SURFACES: USAGE OF NUSSELT CORRELATION EQUATIONS FOR AN INACTIVE, THIN WALLED-TUBE

Antonio Campo* and Alejo Sánchez†

*Department of Nuclear Engineering, Idaho State University, Pocatello, ID 83209, USA; and †Depto. de Ingeniería Mecánica, Universidad de los Andes, Mérida, Edo. Mérida, Venezuela

(*Received* 23 *February* 1997)

Abstract—A semi-analytical analysis was conducted for the prediction of the mean bulk- and interface temperatures of gaseous and liquid fluids moving laminarly at high pressures inside thick-walled metallic tubes. The outer surfaces of the tubes are isothermal. The central goal of this article is to critically examine the thermal response of this kind of in-tube flows utilizing two versions of the 1-D lumped model: one is differential-numerical while the other is differential-algebraic. For the former, the local Nusselt number characterizing an inactive, isothermal tube was taken from correlation equations reported in the heat transfer literature. For the latter, an streamwise-mean Nusselt number associated with an inactive, isothermal tube was taken from standard correlation equations that appear in textbooks on basic heat transfer. In each approach, the combination of the pertinent Nusselt number with the radii ratio of the tube wall and the solid/fluid thermal conductivity ratio, leads to the calculation of either local or mean, equivalent Nusselt numbers, which serve to regulate the thermal interaction between the two dissimilar media. For the two different versions of the 1-D lumped model tested, the computed results consistently demonstrate that the differential-algebraic, provides accurate estimates of both the mean bulk- and the interface temperatures when compared with those temperature results computed with formal 2-D differential models. © 1997 Published by Elsevier Science Ltd.

Keywords—Forced convection, thick-walled tubes, 1-D lumped analysis.

NOMENCLATURE

c_{pf}	specific heat capacity of fluid, J kg^{-1} °C
D_i	inner diameter of tube, m
D_e	outer diameter of tube, m
h	convective heat transfer coefficient, W m^{-2} °C
$\overline{h}$	streamwise mean of h, W m^{-2} °C
k_f	thermal conductivity of fluid, W m^{-1} °C
k_s	thermal conductivity of solid, W m^{-1} °C
K_{sf}	solid/fluid thermal conductivity ratio, k_s/k_f
$\dot{m}$	mass flow rate, kg s^{-1}
Nu	local Nusselt number, Equation 5
$\overline{Nu}$	streamwise-mean of Nu
Nu_{eq}	local, equivalent Nusselt number, U_eD_e/k_f
$\overline{Nu}_{eq}$	streamwise-mean of Nu_{eq}
Pe	Peclet number, $RePr$, $\overline{u}D_i/\alpha_f$
Pr	Prandtl number, ν_f/α_f
q_{wi}	heat flux at the interface, W m^{-2}
Q_T	total heat transfer, W
Q_i	ideal heat transfer, W
r_i	inner radius of tube, m
r_e	outer radius of tube, m
r_r	radii ratio, r_e/r_i
Re	Reynolds number, $\overline{u}D_i/\nu_f$
R_w	dimensionless wall resistance, $\ln(r_r)/(2K_{sf})$
St_{eq}	local, equivalent Stanton number, $Nu_{eq}/RePr$
$\overline{St}_{eq}$	streamwise-mean of St_{eq}
T	temperature,°C
$\overline{u}$	mean velocity of fluid, m s^{-1}

U_e local, overall heat transfer coefficient, W m^{-2} °C
$\overline{U}_e$ mean of U_e, W m^{-2} °C
x axial coordinate, m
X dimensionless x, Equation 5

Greek letters
α_f thermal diffusivity of fluid, m^2 s^{-1}
θ dimensionless T, Equation 5
ν_f kinematic viscosity of fluid, m^2 s^{-1}
ρ_f density of fluid, kg m^{-3}

Subscripts
b mean bulk
e external surface of tube
i internal surface of tube (interface)
o inlet
w wall

INTRODUCTION

In the formulation of problems associated with certain types of specialized applications of in-tube laminar forced convection of high pressure flows, the thermal conductive resistance of the tube wall may be taken as a negligible or a non-negligible quantity, depending on several factors. From a conceptual standpoint, when a uniform temperature is applied at the outer surface of a tube, two extreme possibilities arise. Shah and London [1] explained them by defining a dimensionless thermal conductive resistance as $R_w = \ln(r_r)/(2K_{sf})$. Here, r_r is the radii ratio of the tube wall and K_{sf} is the thermal conductivity ratio between the solid and the fluid media. First, for situations where R_w approaches zero, the thermal behavior of the thick-walled tube logically come near the limiting case of a similar isothermal, but thin-walled tube. Second, for situations where R_w approaches infinity, the heat convection process inside thick tubes tend to that of an opposing limiting case of isoflux, thin-walled tube. These conclusions, of course, were based on observations of the band of local Nusselt number curves, Nu_x, where the family of curves is parameterized by R_w. (see [1, 2]). Except for the previously cited two extreme thermo-geometric conditions, the thermal conductive resistance in dimensionless form, R_w, plays a decisive role in the thermalhydraulic design of thick-walled tubes that clearly needs to be taken into account. Prior to 1978, all the publications devoted to the previously mentioned conjugate, in-tube, laminar convection problem were gathered and compared in the classical monograph of Shah and London [1] and do not need to be repeated here. Actually, these authors pointed out that the two most important works in this specific area are those of Hsu [3] and McKillop *et al.* [4] Hsu [3] alleviated the difficulty caused by a reduced number of eigenquantities available for this problem, determining the first ten eigenquantities by solving the associated Sturm–Liouville equation using a Runge–Kutta integration procedure. He also incorporated implicit asymptotic formulae that facilitated the calculations of higher-order eigenquantities. Subsequently, these formulae enabled Shah and London [1] to accurately evaluate the next 110 eigenquantities and presented tabulated and graphical results for the distributions of local tube Nusselt numbers for representative magnitudes of R_w. Concurrently, McKillop *et al.* [4] analyzed the same problem with a traditional finite-difference method and reported the results in terms of distributions of the local tube Nusselt number as a function of R_w. For practical purposes, their numerical predictions agreed with those of Hsu [3], but were slightly higher.

Understandably, Hsu [3] and McKillop *et al.* [4] tried to present the thermal results in a condensed manner utilizing as a vehicle the traditional local tube Nusselt number format, i.e. $Nu_x = (D_i/k_f)\ (q_{wi}/(T_b - T_{wi}))$. However, by looking at this relation it may be recognized right away that solitary knowledge of the local tube Nusselt number, Nu_x, is insufficient to calculate the actual heat transfer rates, Q_T, in a thick-walled tube of this nature. In addition of the customary Nu_x-distributions, the distributions of the mean bulk and interface temperatures, $T_b(x)$, and $T_{wi}(x)$, are also needed in order to predict the distribution of the interface heat flux, $q_{wi}(x)$. Afterwards, axial integration of $q_{wi}(x)$ gives rise to the precise quantification of Q_T.

Recently, Pozzi and Lupo [5] examined the internal convective problem treated in [3, 4] via an intricate analytical solution which combined an asymptotic series expansion of the Laplace

transform and the stationary-phase method. Their hybrid procedure was quite elaborate and the calculations were carried out in terms of the confluent hypergeometric function. The presentation of results focused on the distributions of the mean bulk and interface temperatures, $T_b(x)$, and $T_{wi}(x)$, exclusively. The results reported in [5] were limited to only two values of the dimensionless wall conductive resistance, R_w, and a reduced tube length.

A complete study accounting for the combined influence of 2-D laminar heat convection in the fluid and the 2-D heat conduction in the annular wall region of a tube was conducted by Campo and Schuler [6]. The applicable conservation equations were solved in a coupled manner using the finite volume method.

Alternatively, this article seeks to address the same 2-D forced convection tube flow reported in refs [3–5] but from a totally different angle. Herein, the outer surface of the thick tube was maintained at a uniform temperature and the solid annular wall itself was considered thermally active. The mathematical model adopted here rests on two versions of a simplistic 1-D lumped-based formulation for the composite fluid-solid domain. Consequently, the present approach deviates considerably from the traditional 2-D differential analyses utilized in refs [3–5]. Incidentally, usage of a 1-D lumped-based formulation led to a simple ordinary differential equation of first order which controls the heat transmission between both media (solid/fluid). This occurs from the origin of the heat exchange region to any downstream station of the thick-walled tube. The resulting 1-D lumped energy equation requires as input data the distributions of either local, or streamwise-mean internal Nusselt number for an identical thermo-fluid situation, but with thermally inactive thin-walled tubes. The determination of the distributions of mean bulk and interface temperatures, $T_b(x)$, and $T_{wi}(x)$, as well as the total heat transfer, Q_T, is carried out in two ways with fast and reliable integrations. The former is numerical and necessitates a Runge-Kutta scheme, whereas the latter is analytical and can be performed by hand or a calculator. With specific reference to ref. [5], the distributions of local Nusselt numbers, Nu_x, are not included in the article, but it may be inferred that calculation of the total heat transfer, Q_T, can be easily achieved via thermodynamic concepts by implementating an overall energy balance between two stations inside the tube.

In synthesis, it is expected that the physically-oriented results obtained in this study will not only provide useful information for theory and applications as well as education in convective heat transfer, but also serve as a complement to the previously cited investigations.

1-D LUMPED-BASED ANALYSES

Conceptually, the formulation of the laminar forced convective problem shown in Fig. 1 may be envisioned as a thermal entrance problem subjected to a conductive exchange between a variable temperature at the inner surface of the tube wall, $T_{wi}(x)$, and the uniform temperature at the outer surface of the tube wall, T_{we}. The thermal boundary condition of uniform temperature is realized in heat exchange devices, for example in condensers and evaporators [1].

Part (a) numerical approach using a variable, convective heat transfer coefficient, h(x)

Under the assumption of constant thermophysical properties for the fluid as well as for the solid wall, a 1-D lumped thermodynamic energy balance applied to a control volume of thickness Δx drawn in Fig. 1 yields;

$$Q_1 = Q_2 + Q_3 \tag{1}$$

In this relation, the nature of the components Q_1 and Q_2 is straightforward, whereas;

$$Q_3 = U_e(\pi D_e)(T_b - T_{we})\Delta x \tag{2}$$

denotes the net rate of heat conducted radially to the external surface of the tube wall at T_{we} from the thermodynamic control volume at T_b. For this particular situation, the local, overall heat transfer coefficient, U_e, is conveniently based on the external diameter of the thick-walled tube, D_e, [7]. That is;

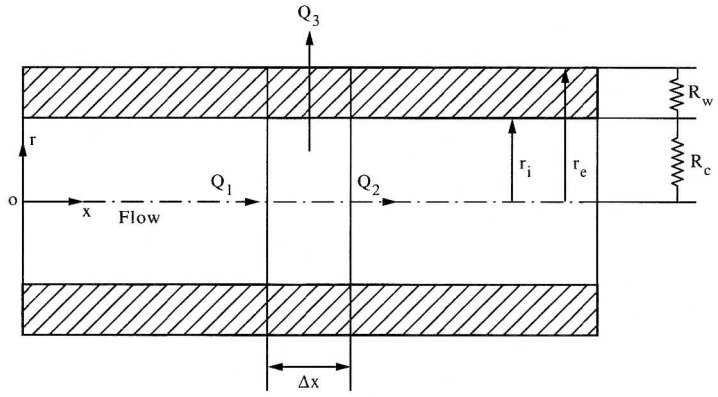

Fig. 1. Schematic diagram of a forced convective flow through a thick-walled tube, the thermal circuit, and the thermodynamic control volume.

$$U_e = \frac{1}{\left(\frac{D_e}{D_i}\right)\frac{1}{h} + \frac{D_e}{2k_s}\ln\left(\frac{D_e}{D_i}\right)} \tag{3}$$

Assuming that axial conduction in both fluid and solid media is negligible, the combination of Equations (1)–(3) supplies the governing 1-D lumped energy equation;

$$\frac{dT_b}{dx} = -4\left(\frac{D_e}{D_i^2}\right)\frac{U_e}{\rho_f c_{pf}\bar{u}}(T_b - T_{we}), T_b(0) = T_0 \tag{4}$$

This is an ordinary differential equation of first order where $\bar{u}$ and T_b designates the mean velocity and the mean bulk temperature of the moving fluid, respectively.

Upon introduction of the customary variables and parameters, both recast in dimensionless form;

$$\theta = \frac{T - T_{we}}{T_0 - T_{we}},\ X = \frac{x}{r_i P_e},\ Nu = \frac{hD_i}{k_f} \tag{5}$$

Equation (3) may be transformed to;

$$U_e = \frac{1}{\frac{D_e}{k_i}\left[\frac{1}{Nu} + \frac{1}{2}\frac{k_f}{k_s}\ln\left(\frac{r_e}{r_i}\right)\right]} \tag{6}$$

Accordingly, Equation (4) may be simplified and rewritten as follows;

$$\frac{d\theta_b}{dX} = -2[N_{eq}(X)]\theta_b, \theta_b(0) = 1 \tag{7}$$

In this equation the local, equivalent Nusselt number, $Nu_{eq} = U_e D_e/k_f$, corresponds to a weighted harmonic mean given by;

$$\frac{1}{Nu_{eq}} = \frac{1}{Nu} + R_w \tag{8}$$

Meanwhile, R_w may be interpreted as the reciprocal of the dimensionless wall conductance of the annular wall, namely $C_w = 1/R_w = 2K_{sf}/\ln(r_r)$, in which the participating quantities are related by;

$$R_w = \frac{\ln r_r}{2K_{sf}}, K_{sf} = \frac{k_s}{k_f}, r_r = \frac{r_e}{r_i} \tag{9}$$

Conversely, for the simpler case pertaining to fully established laminar velocity, uniform entrance temperature, T_0, united to an isothermally inactive thin-walled tube ($T_{we} = T_{wi}$), the heat transfer aspects of the flow may be appropriately characterized by the local Nusselt num-

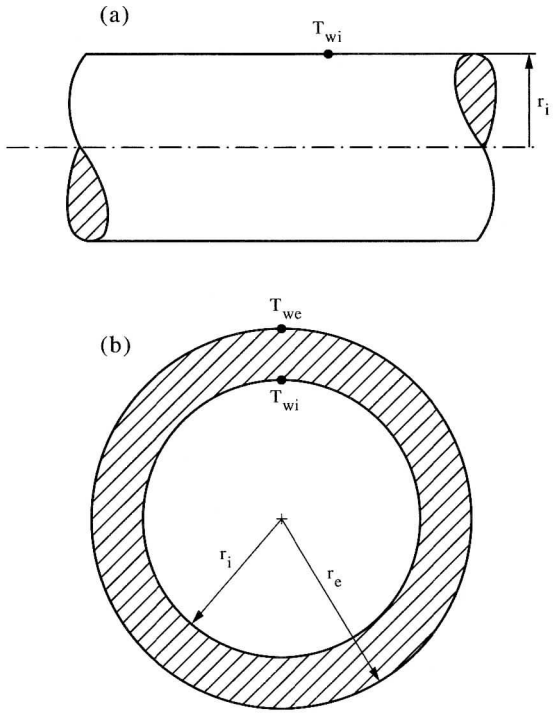

Fig. 2. Two fundamental sub-problems that constitute the input data for the 1-D lumped model: (a) internal forced convection in an isothermal tube; (b) conduction in an annulus.

ber, Nu, as a function of the dimensionless axial position, X. Evidently, this subproblem shown in Fig. 2(a) provides one of the two fundamental solutions for the internal forced convection part. At this point, notice should be taken that a single correlation equation for the local Nusselt number, $Nu(X)$, such as the one constructed by Churchill [8];

$$\frac{Nu+1.7}{5.357}=\left[1+\left(\frac{194}{\pi}X\right)^{-8/9}\right]^{3/8} \tag{10}$$

may be easily incorporated in Equation (8). Also, Shah and London [1] proposed a two-part correlation equation given by;

$$Nu=\begin{cases} 1.357X^{-1/3}-0.7 & \text{for } X\leq 0.02 \\ 3.657+0.331\dfrac{e^{-28.6X}}{X^{0.488}} & \text{for } X>0.02 \end{cases} \tag{11}$$

The other subproblem and its fundamental solution is conceived as merely external, radial conduction in an annular shell of Fig. 2(b) under the influence of a fixed temperature differential.

Naturally, integration of the nonseparable ordinary differential Equation (7) has to be performed numerically with a fourth-order Runge–Kutta algorithm. This procedure produces a numerically determined distribution of the mean bulk temperature, say, $\theta_b(X)$.

Computation of the interface temperatures. In addition to the mean bulk temperature distribution of the fluid, $\theta_b(X)$, the other thermal quantity of comparable interest in heat exchanger applications, is the interface temperature distribution, $\theta_{wi}(X)$. This is especially true for situations where the moving fluid is heated. Obviously, this temperature of local character, may be computed at any station X with the help of two participating thermal resistances. Thus, one possibility involves the local Nusselt number, Nu;

$$\frac{\theta_{wi}}{\theta_b} = \left(1 - \frac{Nu_{eq}}{Nu}\right) \tag{12}$$

Part (b) algebraic approach using a streamwise-mean, convective heat transfer coefficient, $\overline{h}$ (x)

Alternatively, with the objective of avoiding the numerical integration of Equation (7), the use of a simple axially-integrated internal Nusselt number, defined as $\overline{Nu}$

$$\overline{Nu} = \frac{1}{X}\int_0^X Nu dX \tag{13}$$

may be attempted now. Consequently, in this approach the compact correlation equation for the streamwise-mean, internal Nusselt number, $\overline{Nu}$, attributable to Hausen [9]

$$\overline{Nu} = 3.66 + \frac{0.1366X^{-1}}{1 + 0.0635X^{-2/3}} \tag{14}$$

is employed. It should be mentioned that, contrary to Equation (10), Equation (14) constitutes standard material in textbooks of heat transfer (see for instance [7]). Although the conciseness of Equation (14) is adequate, a more compact correlation equation [10] can be constructed as;

$$\overline{Nu} = 3.657 + 1.315X^{-0.366} \tag{15}$$

In view of the foregoing, the systematic step-by-step degradation process of Equation 7 may be started now. The mean, equivalent Nusselt number, $\overline{Nu_{eq}}$, appearing in the right hand side of Equation 7 becomes a single number which clearly emerges from the companion equation to Equation 8;

$$\frac{1}{\overline{Nu_{eq}}} = \frac{1}{\overline{Nu} + R_w} \tag{16}$$

Here, $\overline{Nu}$ has to be evaluated at several pre-determined axial stations X in the downstream portion of the tube. Therefore, with this background in mind, Equation 7 may be transformed into;

$$\frac{d\theta_b}{dX} = -2(\overline{Nu_{eq}})\theta_b, \theta_b(0) = 1 \tag{17}$$

where $\overline{Nu_{eq}}$ is now just a single number. Unquestionably, this ordinary differential equation of first order, classified as separable, is effortless to solve compared to its counterpart nonseparable Equation 7. As expected, this elementary route is advantageous because by merely replacing Nu_{eq} with $\overline{Nu_{eq}}$, the transformed Equation 7, Equation 17, may be readily integrated analytically. This operation yields the compact algebraic expression;

$$\theta_b = \exp(-2\overline{Nu_{eq}} \cdot X) \tag{18}$$

which furnishes the pointwise mean bulk temperature distribution, θ_b (X).

Computation of the interface temperatures

Once the mean bulk temperatures, θ_b (X), were computed, the combination of Equations (14), (16) and (18) enables us to calculate the interface temperatures, θ_{wi} (X), from the relation;

$$\frac{\theta_{wi}}{\theta_b} = \left(1 - \frac{\overline{Nu_{eq}}}{\overline{Nu}}\right) \tag{19}$$

Obviously, this calculation is done in the same manner as before, but now resorting to the streamwise-mean Nusselt numbers, instead of the local Nusselt numbers.

TOTAL HEAT TRANSFER

Attention is now turned to the calculation of the total rate of heat transfer, Q_T, between the fluid stream entering at T_o and the isothermal outer surface of the thick-walled tube. Recall that the tube thickness is designated by the radii ratio, r_r, and the outer surface of the tube was maintained at T_{we}.

Considering the origin, $x = 0$, and any downstream station, say $x = L$ in the fluid domain, Q_T may be determined via a simple overall energy balance as suggested by Jakob [11]. The end result produces the algebraic equation;

$$Q_T = \dot{m}c_{pi}[T_0 - T_b(x = L)] \tag{20}$$

Next, upon introducing an ideal rate of heat transfer, Q_i as;

$$Q_i = \dot{m}c_{pi}(T_0 - T_{we}) \tag{21}$$

a dimensionless heat transfer or thermal efficiency may be recast in compact form as;

$$\frac{Q_T}{Q_i} = 1 - \theta_b \tag{22}$$

Here, it is important to observe that the numerical value of $1 - \theta_b$ is identical to the dimensionless heat transfer.

If the differential/numerical approach is adopted, the computed mean bulk temperature, combined with Equation (22) provides a numerical value for the total amount of heat transfer, Q_T, up to the station $x = L$ in question. In contrast, if the differential/algebraic approach is employed, by virtue of Equation (18) and Equation (22), an analytical expression for the dimensionless total heat transfer;

$$\frac{Q_T}{Q_i} = 1 - \exp\left(-4\overline{St}_{eq} \cdot \frac{L}{D_i}\right) \tag{23}$$

may be readily obtained. Notice that $\overline{St}_{eq} = \overline{Nu}_{eq}/RePr$ stands for the streamwise-mean, equivalent Stanton number which incorporates both the streamwise-mean Nusselt number, $\overline{Nu}_i$, as well as the dimensionless wall resistance, R_w.

It is widely known that the total heat transfer, Q_T, may also be computed indirectly by introducing the traditional tube Nusselt number, Nu_x [12];

$$Nu_x = \frac{D_i}{k_f}\frac{q_{wi}}{(T_b - T_{wi})} \tag{24}$$

However, it should be emphasized that this computational procedure based on convective heat transfer theory is by far more elaborate than Jakob's thermodynamic concept [11] delineated before. From physical grounds, the Nu_x procedure requires an a priori knowledge of the distributions three essential thermal quantities: one of global character, T_b, and the other two of local character, T_{wi} and q_{wi}. In fact, these three quantities have to be reported for selected values of the dimensionless wall resistance R_w (embracing K_{sf} and r_r). As a direct consequence, sole calculation of a band of tube Nu_x-curves has no practical application, other than to establish that the family of Nu_x curves parameterized by R_w is bounded by the two classical distributions for inactive, thin-walled tubes: one for uniform surface heat flux $Nu_{x,H}$ (upper bound for $R_w \to \infty$) and the other for uniform surface temperature $Nu_{x,T}$ (lower bound for $R_w \to 0$), respectively.

In light of the foregoing, the first procedure relying on Equation (22) is quicker and seems to be advantageous for the thermal analyst that needs to make quick decisions with simple calculations. As a by-product, the proposed route for computing Q_T also serves to save journal space in the presentation of results.

DISCUSSION OF RESULTS

With regards to the prevailing criterion for low Peclet number flows, it was recommended that, in general, axial conduction within the fluid stream can be neglected for $Pe > 100$ though there is not a definite consensus on this matter. According to refs [1] and [2] experiments demonstrate that Pe must be higher than 160. This is the limit that was adopted in the present calculations.

Computed results based on the two versions of the approximate 1-D lumped model (for both fluid and solid) will be presented in terms of the distributions of the fluid's mean bulk temperature, θ_b, and the interface temperature, θ_{wi}. The rationale for not presenting the local Nusselt number distributions, i.e. $Nu_x = f(X, R_w)$ for active thick-walled tubes is apparent from Equation (24), and was discussed in detail before.

Examination of the 1-D lumped energy Equation (7) and Equation (17) indicates the presence of four prescribable parameters;

$$Re, Pr, r_r, K_{sf} \tag{25}$$

and from dimensional analysis, it is evident that they can be grouped together. For instance, as is customarily done in the analysis of laminar flows inside thin-walled tubes, the Peclet number, Pe, can be absorbed by the dimensionless axial coordinate X, as shown in Equation (5). As a result, the respective geometric and thermal parameters r_r and K_{sf} can be merged with the purpose of identifying a single dimensionless wall conductive resistance, namely R_w, in Equation (9).

As a preliminary test, the validity of the 1-D lumped model and their numerically- and algebraically-determined solutions will be demonstrated for an extreme situation of forced convection through a comparable isothermally, inactive thin-walled tube. Inspection of Fig. 1 reveals that in the limit dictated by a large value of the dimensionless wall conductive resistance, R_w, the inner surface temperature, T_{wi}, coincides with that of the outer surface temperature, T_{we}. This extreme situation is manifested by the presence of only one conductive resistance, i.e. the fluid conductive resistance and of course ensures the respective simplifications of $Nu_{eq}(X)$ into $Nu(X)$ in Equation (8) and $\overline{Nu}_{eq}$ into $\overline{Nu}$ in Equation (16). Therefore, introducing Equation (10) into Equation (7) and Equation (14) into Equation (17) successively the mean bulk temperature distributions linked to an isothermal, inactive thin-walled condition must be recovered. Figure 3 attests the accuracy of the mean bulk temperature values supplied by the two solution methods (one numerical and the other algebraic) for the 1-D lumped model when compared with the benchmark results of the 2-D differential model taken from Table 13 in Shah and London [1]. For practical purposes, the deviations between the three curves are nonexistent.

Table 1 illustrates typical magnitudes of the solid/fluid thermal conductivity ratio, K_{sf}, at two different temperatures for real combinations of solids and fluids employed in tubes for heat exchange devices. The ratios range approximately from 0.16 (steel tube/sodium flow) to 16000 (copper tube/air flow) spanning five orders of magnitude. Further, Table 2 displays typical values of the radii ratios, r_r, of steel tubes currently employed in the construction of tubular heat exchangers. Analogous tables are obtainable for other metallic tubes, but are not presented here.

In view of the foregoing, the discussion of results will be focused on the goodness of the approximate numerical and algebraic evaluations of the 1-D lumped model as well as its comparison with the formal and more rigorous analytical solution of the 2-D differential model. For the latter, the set of recently published results by Pozzi and Lupo [5] will be employed as a baseline solution. These authors, relying on the confluent hypergeometric function, presented tabulated and graphical results for two cases wherein the dimensionless wall conductive resistance, R_w was taken as 0.5 and 5, respectively. In passing, it should be stressed that the physics of this conjugate, forced convection problem is well understood (Shah and London [1]) and consequently will not be explained here.

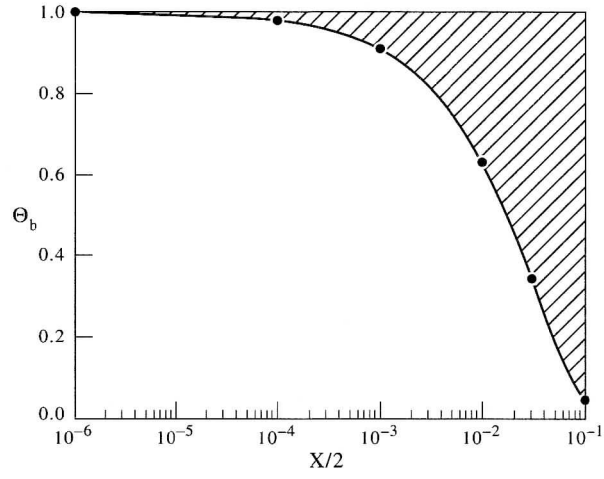

Fig. 3. Comparison of the fluid's mean bulk temperature distribution for the limiting case of an isothermal, inactive thin-walled tube (•, Shah and London [1]; ———, Present Runge–Kutta and algebraic calculations).

Part (a) numerical lumped approach

Figure 4 displays the mean bulk- and the interface temperature distributions for $R_w = 5$, which is the highest magnitude selected in the study by Pozzi and Lupo [5]. To inject some practicality into this thermogeometric dimensionless group, the value of 5 may be conceived for example as a combination of a solid/fluid thermal conductivity ratio of $K_{sf} = 1.8$ and a wall radii ratio of $r_r = 1.2$. In the figure, the solid lines correspond to the results produced by the 1-D lumped model and the Runge–Kutta integration of Equation (7), whereas the rectangles identify the analytical values reported by Pozzi and Lupo [5]. As may be seen, the numerically-determined mean bulk temperatures, θ_b, (or its equivalent total heat transfer rates, are plotted in the upper part of the figure and overlap the predictions obtained analytically in [5]. Meanwhile, the interface temperatures, θ_{wi}, occupy the bottom part of the figure and the exhibited deviations are indeed trivial. For the latter, the discrepancies are more pronounced near the origin of the heat exchange section but tend to be attenuated as the fluid moves toward the downstream region. This behavior is understandable because of the sensitivity of the interface temperatures (local quantities). Further comparisons for stations located at $X < 2 \times 10^{-6}$ and at $X > 2 \times 10^{-3}$ were not possible because neither global nor local temperatures were reported by Pozzi and Lupo [5].

Part (b) algebraic lumped approach

Additionally, it may also be observed in Fig. 4 that the algebraically-obtained mean bulk temperature (or its equivalent heat transfer rate) shows excellent agreement with the exact values computed by Pozzi and Lupo [5], whereas the magnitudes of the interface temperatures are slightly overpredicted. As may be seen, the largest relative error for this local temperature occurs near the origin. In particular, at the station $X = 2 \times 10^{-6}$ the deviation is synonymous of a relative error of 5%. Thereafter, the errors tend to decay gradually as the fluid moves toward the downstream region. Further comparisons beyond the station $X > 2 \times 10^{-3}$ were not possible because temperatures at these locations were not reported by Pozzi and Lupo [5].

Table 1. Combinations of practical solid/fluid thermal conductivity ratios, K_{sf}.

	Sodium	Water	Oil	Air
Copper	4.64	665	2660	15960
Aluminum	2.74	393	1573	9440
Iron or Nickel	0.94	135	540	3240
Steel or Tunsgten	0.16	23	93	560

Table 2. Radii ratios of steel tubes for heat exchangers (adapted from Ref. [7]).

Outside diameter (mm)	Radii ratios				
	1.20	1.60	2.00	2.60	3.20
16	1.18	1.25	1.33		
20		1.19	1.25	1.35	
25		1.15	1.19	1.26	1.34
30		1.12	1.15	1.21	1.21
38			1.12	1.16	1.20

Criterion for considering thick-walled tubes

Figures 5 and 6 were prepared to show the underlying heat transfer characteristics of moderate thick-walled tubes parameterized by the dimensionless wall resistance, R_w, where the numerical values chosen cover the ample range of $0.001 < R_w < 1$.

Attention is first turned to Fig. 5 illustrating the variation of the mean bulk temperature θ_b, (a global quantity) with X. In fact, this set of curves also provides parallel information with regards to the total heat transfer caused by the existing interlink between θ_b and the dimensionless heat transfer, as evidenced in Equation 22. As a result of the relatively large value of $R_w = 1$, the first curve varies rather slowly with the axial coordinate, X, clearly resembling the trend associated with that of an isoflux boundary condition at an inactive thin-walled tube. The maximum value of R_w selected for this figure is one of convenience in order to demonstrate clearly the distortion of the θ_b-temperatures. Next, when intense heat conduction is brought into the picture by decreasing R_w ten times to $R_w = 0.1$, the second θ_b-curve drops off more rapidly and the cooling is intensified. This sweeping pattern persists for $R_w = 0.01$ in which the slope of the curve is more pronounced and the θ_b-distribution has a shorter size. Beyond $R_w = 0.01$ changes in the magnitude of θ_b becomes of lesser importance and the corresponding subfamily of θ_b-curves for $0.001 < R_w = 0.01$ tends to stabilize. Owing to the proximity of these curves in Fig. 5 as R_w diminishes, it may be inferred that an accurate criterion that establishes the borderline between a thin-walled and thick-walled tubes may be obtained. This borderline may be associated with the magnitude of the dimensionless wall resistance given by $R_w = 0.001$.

In fact, the θ_b-curve for $R_w = 0.001$ coincides with the mean bulk temperature distribution corresponding to the classical Graetz solution (Shah and London [1]) which is indicated by solid circles. Recall that the latter is valid for inactive, isothermal thin-walled tubes; in other words $R_w \to 0$. A detailed inspection of these two θ_b-curves confirms that the agreement is excellent.

Under these premises, whenever $R_w \leq 0.001$ the mean bulk temperature can be safely computed from the correlation equation [10]

$$\ln \theta_b = 0.0036 - 5.4787X - 1.2514X^{0.5} \tag{26}$$

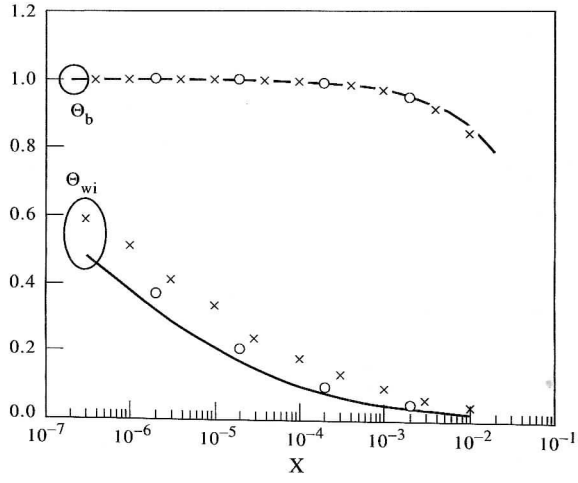

Fig. 4. Comparison of the fluid's mean bulk and interface temperature distribution for $R_w = 5$ (○, Pozzi and Lupo [5]; ———, Present Runge–Kutta calculations; and ×, Present algebraic calculations).

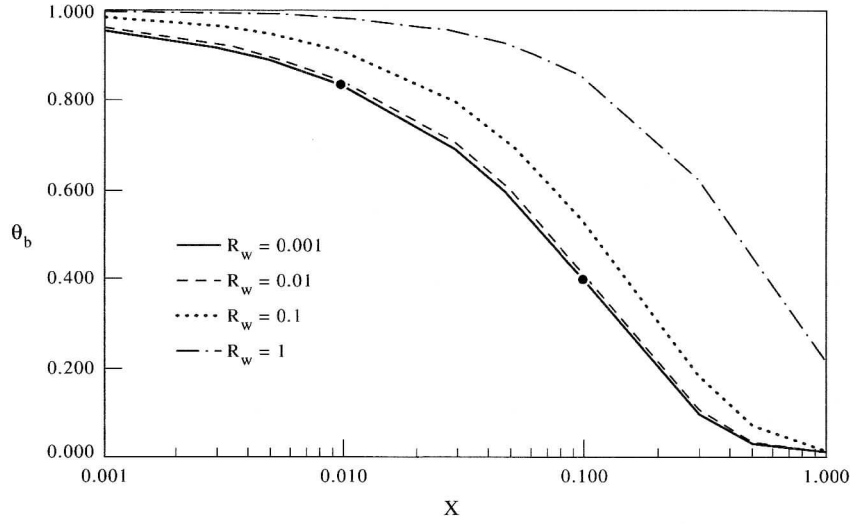

Fig. 5. Variation of the fluid's mean bulk temperature parameterized by the dimensionless wall resistance (•, limiting case of an isothermal thin-walled tube, Shah and London [1]).

which corresponds to the limiting case of thin-walled tubes dictated by $R_w = 0$, i.e. the classical Graetz solution.

Further, this information is better presented in Fig. 6 which displays the companion interface temperature distribution parameterized by R_w. Compared with Fig. 5, the distortions of the interface temperature distributions, θ_{wi}, as expected are more notorious and the curves are separated. As mentioned in the previous paragraphs, in the first case for $R_w = 1$ the magnitude of θ_{wi} in the immediate vicinity of the origin of the heat exchange region, reaching a value of 0.95 at $X = 0.001$. This behavior responds to a large value of R_w where the axial temperature difference across the annular solid wall is accentuated in the downstream region, but not in the upstream region. For the second curve associated with $R_w = 0.01$ the interface temperature reaches a value of 0.7 at the entrance and thereafter is slightly disfigured. The linear slope of this curve in semi-log coordinates is also observed in the figure.

Conversely, the third θ_{wi}-curve for $R_w = 0.01$ in the family of curves exhibits a value of almost 0.2 at $X = 0.001$ and decreases gradually in the downstream direction. Except for the immediate vicinity of $X = 0$, the shape of this curve reflects a quasi-asymptotic isothermal condition at the wall. For $R_w = 0.01$, the local nature of the interface temperature still impedes the concordance

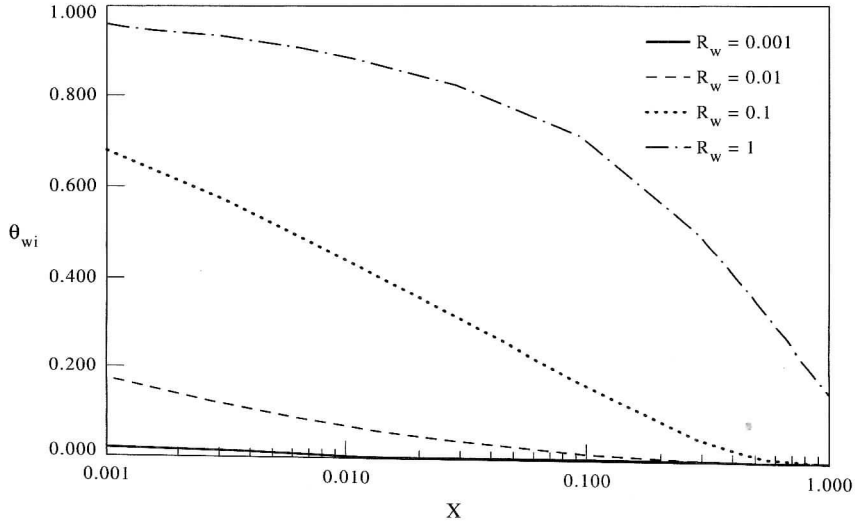

Fig. 6. Variation of the interface temperature distribution parameterized by the dimensionless wall resistance.

of the θ_{wi}-curve with the abscissa (dictated by $\theta_{wi}=0$), This behavior is in marked contrast with the almost perfect agreement observed for the corresponding θ_b-curve. Finally, the culmination of the information developed so far is presented in the last θ_{wi}-curve. Here, it is immediately noticeable that this curve describing the magnitude of $R_w=0.001$ is much flatter. Essentially, the interface temperature experiences a substantial decrease in the vicinity of $X = 0$. In particular, the curve does coincide with the abscissa for all practical purposes because the mismatch at $X = 0.001$ is around 0.02 units. Here again, this unique feature corroborates the adequacy of the aforementioned threshold between thin- and thick-walled tubes, namely $R_w=0.001$. This aspect indeed constitutes an alternate interpretation which is explained in the forthcoming paragraphs.

As already mentioned, Table 1 provides the numerical values of K_{sf} for typical combinations of solids and fluids in heat exchanger tubes. Next, it was decided to construct a companion table, Table 3 in order to display the corresponding values of the radii ratio r_r of the tubes that have to be exceeded for the implementation of the computational procedure for thick-walled tubes proposed here.

The definition of the dimensionless wall resistance, $R_w=\ln r_r/(2\ K_{sf})$, permits us to separate the influence of the geometric parameter, that is the radii ratio r_r from the effect of the thermal parameter, i.e. the thermal conductivity ratio, K_{sf}. This decoupled approach eventually yields the inequality;

$$r_r > 0.002K_{sf} \tag{27}$$

which is connected to the thick-walled tube analysis.

Inspection of Table 3 reveals some interesting features and trends of the physics of fluids. For instance, for sodium flow, the thick-tube analysis must be employed regardless of the nature of the solid metal. This feature is indicative of the dominance that the geometric parameter exerts over the companion thermal parameter. These situations are solely controlled by the former parameter. Next, for water flows a trade-off between the geometric and thermal parameters is manifested. Focusing the attention on the copper/water combination, it can be seen that whenever $r_r < 3.80$ the simple thin tube approximation is valid. On the contrary, when this value is surpassed, the thick tube analysis has to be brought over. Moving down to the column for water, the magnitudes of r_r tends to diminish in accordance with the existing proportionality between r_r and K_{sf}. For specific situations wherein the moving fluid is oil two contrasting cases show up. First, when the metal is copper or aluminum, the thin tube approximation holds irrespective of the thickness of the tube wall. Second, for tubes fabricated from iron, nickel, steel and tungsten a competition between the geometric and thermal parameters is evident. The trends observed for oil persist for air flows but they are a bit more pronounced. Finally, suffice it to say that any metallic tube transporting air can be treated as a thin tube approximation with the exception of steel and tungsten. In fact, for these two metals the thin tube limit is applicable as long as $r_r < 3.10$.

The exhaustive examination described in the preceding paragraphs relying exclusively on primitive variables, such as r_r and K_{sf} rather than a derived dimensionless group, R_w, can be utilized as guidelines by thermal design engineers as well as students in courses of thermal engineering.

CASES FOR SIMULTANEOUS FLOW AND TEMPERATURE

The theoretical and applied aspects of this article may be easily extended to more complex situations involving simultaneous development of laminar flow and temperature. The fluids

Table 3. Values of the radii ratios, r_r, where the active thick-walled treatment has to be accounted for.

	Sodium	Water	Oil	Air
Copper	> 1.01	> 3.80	Very large	Very large
Aluminum	> 1.00	> 2.20	Very large	Very large
Iron or Nickel	> 1.00	> 1.30	> 3.00	Very large
Steel or Tungsten	> 1.00	> 1.05	> 1.20	> 3.10

move through active thick-walled tubes with imposed temperature at the outer surface possessing intermediate-to-large Prandtl numbers.

Initially, Kays [12] had recommended that for fluids characterized by $Pr > 5$, the laminar velocity profiles develop so much faster than the temperature profile that the assumption of fully developed velocity at the tube entrance ($X = 0$) seems to be reasonable and thereby introduces little error. Within this context, recent calculations by Shome and Jensen [13] have convincingly demonstrated that for high-Prandtl-number fluids, i.e. $Pr > 50$, the simultaneous laminar flow and temperature may be modelled without loss of accuracy by a limiting case accounting for fully developed parabolic velocity. To this effect, the correlation equation;

$$\frac{\overline{Nu}}{\overline{Nu}(Pr = \infty)} = [1 + 0.035(PrX)^{-0.88}]^{0.17} \tag{28}$$

was developed in [13] where the denominator of the left hand side corresponds to Equation (14). Consequently, directing the attention to the third column of Table 1 reveals that oils and organic fluids characterized by $Pr > 50$ possess high thermal conductivity ratios that are of the order of $K_{sf} \geq 100$.

CONCLUDING REMARKS

In this article, simple yet reliable numerical and algebraic computational methods were developed and tested for the problem of fluid-to-solid heat transfer in thick-walled tubes with isothermal conditions at the outer surface. Resting on a simple 1-D lumped model for laminar regimes, the distributions of both, mean bulk- and interface temperature, may be computed by implementing a fourth-order Runge-Kutta algorithm or by evaluating a position-dependent exponential function by hand or with a calculator. Comparison of the total heat transfer magnitudes with analytically-determined solutions for a 2-D distributed formulation convincingly demonstrates that the present 1-D lumped methodology gives results of excellent accuracy.

In view of its simplicity, it appears that the proposed 1-D approach possesses some inherent advantages for the analysis of this class of laminar heat convection problems. Likewise, it serves to complement complex 2-D differential models that inevitably need to be solved by sophisticated numerical procedures, like the finite difference method on a personal computer or workstation.

REFERENCES

1. R. K. Shah and A. A. London, *Laminar Flow Heat Transfer in Ducts*. Academic, New York, NY (1978).
2. R. K. Shah and M. S. Bhatti, Laminar Convective Heat Transfer in Ducts. In *Handbook of Single-Phase Convective Heat Transfer*, (Edited by S. Kakac *et al.*). Wiley, New York, NY (1987).
3. C. J. Hsu, Laminar flow heat transfer in circular or parallel-plate channels with internal heat generation and the boundary condition of the third kind. *J. Chinese Inst. Chem. Engng.* **2,** 85–100 (1971).
4. A. A. McKillop, J. C. Harper and P. E. Peck, Heat transfer in entrance region flow with external resistance. *Int. J. Heat Mass Trans.* **14,** 863–866 (1971).
5. A. Pozzi and M. Lupo, The coupling of conduction with forced convection in Graetz problems. *J. Heat Trans.* **112,** 323–328 (1990).
6. A. Campo and C. Schuler, Coupled analysis of fluid-to-solid laminar heat transfer in thick-walled short tubes with uniformly imposed temperature. *Numer. Heat Trans., Part B, Applications* **20,** 237–252 (1991).
7. A. F., Mills, *Heat Transfer*. Richard Irwin, Boston, MA, p. 70 and p. 847 (1992).
8. S. W. Churchill and H. Ozoe, Correlations for laminar forced convection in flow over an isothermal flat plate and in developing and fully developed flow in an isothermal tube. *J. Heat Trans.* **95,** 416–420 (1973).
9. H. Hausen, Darstellung des Warmeuberganges in Rohren durch verallgemeinerte Potenzbeziehungen. *Z. VDI Beih. Verfahrenstech* **4,** 91–96 (1943).
10. A. Campo, Class notes on Heat Transfer, 1995.
11. M. Jakob, *Heat Transfer*. Vol. I, McGraw Hill, New York, NY (1949).
12. W. M. Kays, *Convective Heat Transfer*. 1st edition, McGraw-Hill, New York, NY (1966).
13. B. Shome and M. K. Jensen, Correlations for simultaneous developing laminar flow and heat transfer in a circular tube. *Int. J. Heat Mass Trans.* **36,** 2710–2713 (1993).